ACS APPLIED MATERIALS & INTERFACES

Research Article

www.acsami.org

Phenylboronic-Acid-Modified Nanoparticles: Potential Antiviral Therapeutics

Manakamana Khanal,[†] Thibaut Vausselin,[‡,§,∥,⊥] Alexandre Barras,[†] Omprakash Bande,[#] Kostiantyn Turcheniuk,[†,▽] Mohammed Benazza,[#] Vladimir Zaitsev,[○] Cristian Mihail Teodorescu,[◆] Rabah Boukherroub,[†] Aloysius Siriwardena,[*,#] Jean Dubuisson,[*,‡,§,∥,⊥] and Sabine Szunerits[†,*]

[†]Institut de Recherche Interdisciplinaire (IRI, USR CNRS 3078), Université Lille 1, Parc de la Haute Borne, 50 Avenue de Halley, BP 70478, 59658 Villeneuve d'Ascq, France

[‡]Center for Infection & Immunity of Lille (CIIL), Institut Pasteur de Lille, F-59019 Lille, France

[§]Inserm U1019, F-59019 Lille, France

[∥]CNRS UMR8204, F-59021 Lille, France

[⊥]Université de Lille Nord de France, F-59000 Lille, France

[#]Laboratoire des Glucides (FRE 3517 CNRS), Université de Picardie Jules Vernes, 33 rue saint Leu, 80039 Amiens, France

[▽]Departement of Fine Organic Synthesis, Institute of Bioorganic Chemistry and Petrochemistry NAS of Ukraine, 1 Murmanska Str., 02660 Kiev, Ukraine

[○]Taras Shevchenko University, 60 Vladimirskaya str., Kiev, Ukraine

[◆]National Institute of Materials Physics, Atomistilor 105 bis, 077125 Magurele, Romania

ABSTRACT: Phenylboronic-acid-modified nanoparticles (NPs) are attracting considerable attention for biological and biomedical applications. We describe here a convenient and general protocol for attaching multiple copies of *para*-substituted phenylboronic acid moieties onto either iron-oxide-, silica- or diamond-derived NPs. The boronic acid functionalized NPs are all fabricated by first modifying the surface of each particle type with 4-azidobenzoic ester functions. These azide-terminated nanostructures were then reacted with 4-[1-oxo-4-pentyn-1-yl) amino]phenylboronic acid units via a Cu(I) catalyzed Huisgen cycloaddition to furnish, conveniently, the corresponding boronic-acid modified NPs (or "borono-lectins") targeted in this work. The potential of these novel "borono-lectins" as antiviral inhibitors was investigated against the Hepatitis C virus (HCV) exploiting a bioassay that measures the potential of drugs to interfere with the ability of cell-culture-derived JFH1 virus particles to infect healthy hepatocytes. As far as we are aware, this is the first report that describes NP-derived viral entry inhibitors and thus serves as a "proof-of-concept" study. The novel viral entry activity demonstrated, and the fact that the described boronic-acid-functionalized NPs all display much reduced cellular toxicities compared with alternate NPs, sets the stage for their further investigation. The data supports that NP-derived borono-lectins should be pursued as a potential therapeutic strategy for blocking viral entry of HCV.

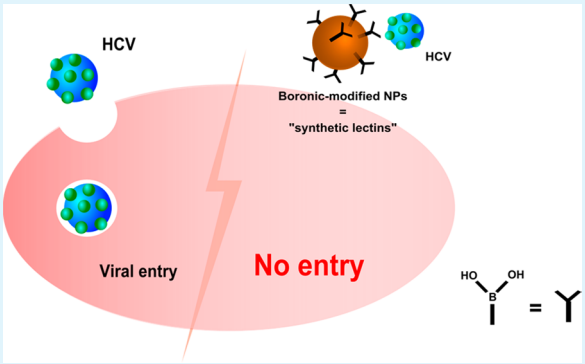

KEYWORDS: *Hepatitis C virus, synthetic lectin, diamond nanoparticles, magnetic nanoparticles, silica particles, "click" chemistry, boronic acid*

1. INTRODUCTION

The development of functional nanoparticles (NP) for biological and biomedical applications has attracted great interest during the past decade.[1−4] Solutions to several of the recurrent problems associated with drug administration have been addressed using NP-based strategies, and this has seen a countless number of functionalized NPs being developed and examined for such purposes.[1] Many of these drug-conjugated nanostructures have been reported to be more efficient than the active drug alone. This increased affinity has often been attributed to the presence of multiple copies of the particular drug on the nanoparticle surface.[2,5] A ligand-type that has received considerable attention in medicinal chemistry is boronic acid.[6,7] The ability of boronic acid moieties to form tetravalent boronate diester cyclic complexes selectively and reversibly with either 1,2- or 1,3-*cis*-diols, such as those typically present in saccharides, is well-known.[8] These "pseudo-lectins" or "borono-lectins", as they have sometimes been called

Received: September 3, 2013
Accepted: November 1, 2013
Published: November 1, 2013

(because of their affinity for carbohydrates), have previously been investigated for the specific capture of glycoproteins from unfractionated protein mixtures.[9−12] Other recent examples of the use of boronic-acid-modified NPs include the target-selective photodegradation of oligosaccharides by fullerene-boronic acid hybrids upon visible light irradiation,[13] or the glucose-responsive release of insulin and cyclic adenosine monophosphate (cAMP) from boronic-acid-modified mesoporous silica nanoparticles.[14] The rate of formation/dissociation of such phenylboronate diester complexes is in addition pH-dependent and occurs most rapidly when boron is tetrahedral, which is favored at higher pH values.[15,16] Variations in the structures of the phenylboronic acid unit can give analogues with improved affinity and selectivity toward a given saccharide as well as analogues with modulated pH optima, better adapted for sequestering sugars under physiological conditions.[6,17−19]

Boronic-acid-derived molecules have more recently been proposed as a potential therapeutic strategy for the treatment of Human Immunodeficiency virus (HIV), and the activity of these compounds has been attributed to their affinity to bind to the highly glycosylated envelope of this virus.[20−22] Investigations have shown a general lack of activity of monovalent phenylboronic acid derivatives toward HIV.[23] When significant numbers of phenylboronic acid moieties are presented on a polymeric scaffold, these multivalent analogues have been demonstrated to more effectively interfere with interactions of HIV with its target host cells and thereby reduce viral infection.[22,24,25] The success of the boronic-acid-containing polymers has been attributed to their ability to form multivalent interactions with viral glycans. The polymers can form multiple phenylboronate diester complexes with the multiple *cis*-diol units present on the glycans of glycosylated envelope of HIV, whereas the corresponding monovalent boronic acids cannot.

Surprisingly, the potential of multivalent boronic-acid-derived edifices to block viral entry has not been validated as a therapeutic strategy for Hepatitis C virus (HCV) up until now. Such compounds would a priori have potential for blocking HCV entry, as like HIV this virus also features highly glycosylated envelope proteins. Furthermore, the presence of these N-linked surface glycans has been shown to modulate the accessibility to some of its receptors.[26−28] Preferential infection of the liver by HCV results in the establishment of chronic infection in the majority of cases and can lead to cirrhosis and hepatocellular carcinoma over the course of several years.[29] Among the handful of molecules reported to show HCV viral entry inhibitory activity are included a variety of glycan recognizing proteins (GBPs or lectins)[30] as well as natural products such as pradimicin.[31,32] Proteins such as cyanovirin-N and griffithsin have been shown conclusively to owe their activity to their interaction with high-mannose glycans present on HCV envelope glycoproteins.[31,33] However, the high costs of large-scale production and purification of these protein-based antivirals together with their low stability, vulnerability to proteolytic cleavage, as well as their mitogenicity undermines their eventual use. The concept of using nonpeptidic carbohydrate binding agents such as pradimicin for HIV viral inhibition has been proved using HIV-exposed Simian macaque models and HCV-infected chimeric mice that harbor primary human hepatocytes in the liver. The natural mannose-binding product pradimicin showed HCV entry inhibition that fueled hope that synthetic molecules that bind glycans strongly and selectively might be alternatives to antiviral lectins and moreover better-adapted for use in a clinical setting.[34,35]

In the present study, we have selected to investigate phenylboronic-acid-modified NPs for their HCV viral entry inhibition potential. Boronic-acid-based NP are expected to benefit from a number of advantages over other current HIV inhibitors including being inexpensive to produce and purify, more stable over a long time as well as not being mitogenic. In addition, when multiple copies of an appropriate boronic acid derivative are grafted onto a scaffold, the affinity from glycosylated enveloped virus surfaces should be significantly increased compared with that of the starting monomer. This increase is consistent with multiple grafted boronic acid moieties reacting simultaneously with several diol units on the same monosaccharide or with multiple diol units spanning over the length of an entire oligosaccharide (or adjacent oligosaccharide units). Herein, we describe the first examples of NPs, specifically engineered to behave as HCV entry inhibitors (Figure 1). It was considered prudent to target compounds

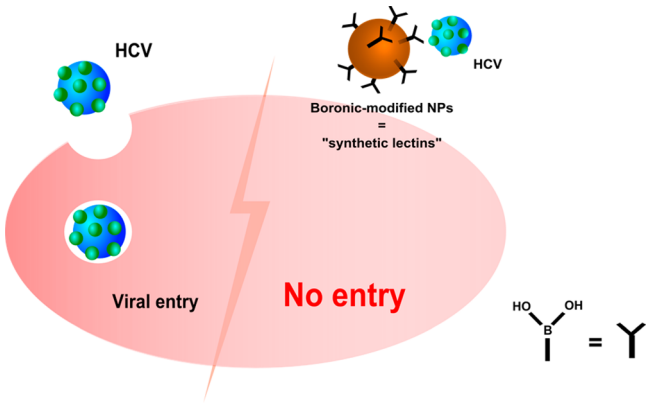

Figure 1. Schematic drawing of the underlying concept of using boronic-acid-modified nanoparticles as HCV entry inhibitors.

based on a variety of starting nanomaterials in the initial phase of the present study, in the knowledge that the viral entry inhibitory properties of any NP-derived boron-lectin would probably be related intrinsically to their particular physiochemical properties as well as to their molecular dimensions. The choice of the three different particles, magnetic, silica and diamond NPs used in this study was arbitrary and guided mainly by the successful use of these particles for other biomedical applications.[1,36−39] Neither the magnetic properties nor the fluorescent properties of nanodiamonds were used in this present study, as the main focus was on the development of a common surface strategy for the formation of NP-derived borono-lectins. Particles such as magnetic- (MPs),[10,40,41] silica- (silica-NPs),[11] and nanodiamond (ND),[20−22,42,43] featuring multiple surface-conjugated boronic acid groups, have already been investigated for their ability to capture glycoproteins but have not previously been considered as HCV viral entry inhibitors.[1] The Cu(I) catalyzed azide−alkyne cycloaddition conjugation reaction was selected in this work for the synthesis of boronic acid modified NPs in the knowledge that "click" strategies are now widely used in chemistry and biology due to their well-described attributes[44,45] such as chemoselectivity and mildness of reaction conditions.

2. EXPERIMENTAL SECTION

Materials. Ammonium hydroxide, iron(II) chloride tetrahydrate ($FeCl_2{\cdot}4H_2O$), iron(III) chloride hexahydrate ($FeCl_3{\cdot}6H_2O$), 4-(bromomethyl)-phenylboronic acid, 3-(bromomethyl)-phenylboronic acid, 4-aminophenylboronic acid hydrochloride, 4-pentynoic acid, *N*,*N*′-dicyclohexylcarbodiimide (DCC), 4-dimethylaminopyridine (DMAP), ethylenediaminetetraacetic acid (EDTA), triethylamine, copper iodide (CuI), anhydrous ethanol, dimethylformamide (DMF), 3-hydroxytyramine hydrochloride, sodium nitrite, sulfuric acid (H_2SO_4), sodium hydroxide (NaOH), anhydrous acetonitrile, 4-aminopropyltrimethoxysilane (APTMS), and silicon dioxide nanopowder (10−20 nm particle size (BET), Nr. 637238, silica NP) were obtained from Sigma-Aldrich and used without any further purification. 4-Azidobenzoic acid was purchased from TCI Europe, Belgium. Hydroxylated diamond particles (ND-OH particles) were obtained from the International Technology Centre, Raleigh, NC.

$CuI(PPh_3)$ was synthesized as described in the literature.[46] In short, a solution of triphenylphosphine (0.69 g, 2.63 mmol) in 10 mL of acetonitrile was added to a solution of CuI (0.50 g, 2.63 mmol) in the same solvent (50 mL). A complex started to precipitate after a few seconds. The mixture was stirred for 1 h and then the precipitate was filtered, washed with acetonitrile, and vacuum-dried (yield 80%).

Synthesis of 4-[(1-Oxo-4-pentyn-1-yl)amino]phenylboronic Acid (1). Compound **1** was synthesized according to the literature with some modifications.[47] 4-Pentynoic acid (150 mg, 1.5 mmol) was dissolved in water (5 mL), and the pH of the solution was adjusted to 4.8 with a 0.1 N NaOH solution. 4-Aminophenylboronic acid hydrochloride (312 mg, 1.8 mmol) was dissolved in water (5 mL) in a round-bottom flask, and the pH value of the solution was adjusted to 4.8 using 0.1 N NaOH. EDC (345 mg, 1.8 mmol) was added, and the solution was stirred at 0 °C for 20 min. Then 4-pentynoic acid solution was slowly added to the reaction medium with a syringe, and the reaction mixture was incubated for 1 h in ice, and afterward overnight at room temperature. White precipitate appeared and was collected by filtration. The solid was washed with water (3 times) and finally oven-dried at 50 °C for 24 h. The product was isolated as a white solid (260 mg, yield 67%). ^{1}H NMR (300 MHz, DMSO-d_6): δ 10.00 (s, 1H, O═CNH), 7.91 (s, 2H, B−OH), 7.71 (d, J = 8.1 Hz, 2H, Ar−H), 7.55 (d, J = 8.1 Hz, 2H, Ar−H), 2.81 (t, J = 2.5 Hz, 1H, HC≡CR), 2.6−2.4 (m, 4H, $-CH_2-CH_2-$)

Synthesis of 2-Nitrodopamine (2). 3-Hydroxytyramine hydrochloride (1.90 g, 10 mmol) and sodium nitrite (1.52 g, 22 mmol) were dissolved in water (25 mL) and cooled to 0 °C. Sulfuric acid (17.4 mmol in 10 mL of water) was added slowly to the mixture, and a yellow precipitate was formed. After stirring overnight at room temperature, the precipitate was filtered and recrystallized from water to give a product as a hemisulfate salt.[48] Yield 1.9 g (77%). ^{1}H NMR (300 MHz, DMSO-d_6): 7.47 (s, 1H, Ar−H), 6.85 (s, 1H, Ar−H), 3.10 (br s, 4H, $-CH_2-CH_2-$). The product was purified through a column with Dowex ion-exchange resin to get free amine as reddish solid.

Formation of Boronic-Acid-Modified Particles. *Silica Particles.* Amine-terminated silica particles (silica-NH_2) were prepared by sonicating silica NPs (60 mg) for 30 min in anhydrous ethanol (20 mL), and then APTMS (6 μL) was added and the suspension was stirred for 24 h at room temperature under nitrogen. Silica-NH_2 was obtained by three consecutive wash/centrifugation cycles at 12 300 rcf (Scanfuge Mini, ORigio). The purified particles were oven-dried at 50 °C overnight.

4-Azidobenzoic acid (0.20 mmol), DCC (0.22 mmol), and DMAP (0.066 mmol) were dissolved in 5 mL of anhydrous DMF. A suspension of silica-NH_2 in anhydrous DMF (10 mg in 5 mL) was added to the solution, and the mixture stirred at room temperature for 24 h under nitrogen. The azido-terminated silica particles (silica-N_3) were isolated through consecutive wash/centrifugation at 12 300 rcf with DMF (twice) and ethanol (twice) and finally oven-dried at 50 °C overnight.

The silica-N_3 (15 mg) were dispersed in 15 mL of anhydrous DMF and sonicated for 40 min. The "click" reaction was carried out by addition of 4-[(1-oxo-4-pentyn-1-yl) amino]phenylboronic acid (**1**) (4 mM) and $CuI(PPh_3)$ (0.4 mM) to the silica-N_3 suspension and stirred for 48 h at 80 °C. The resulting nanoparticles were separated by centrifugation at 12 300 rcf, purified through consecutive wash/centrifugation cycle at 12 300 rcf with DMF (twice) and 1 mM EDTA water solution (twice), and finally oven-dried at 50 °C overnight.

Magnetic Particles. Water dispersion of bare iron magnetic nanoparticles (10 mg/mL, 1 mL), formed as reported previously,[49] was mixed with 2-nitrodopamine (7 mg) and sonicated for 1 h at room temperature. The modified particles (MP-NH_2) were isolated by means of a magnet and purified through six consecutive wash/precipitation cycles at 12 300 rcf with water to ensure complete removal of unreacted amine.

4-Azidobenzoic acid (0.20 mmol), DCC (0.22 mmol), and DMAP (0.066 mmol) were dissolved in 5 mL of anhydrous DMF and stirred for 1 h at room temperature. A suspension of MP-NH_2 was added, and the resulting mixture was stirred overnight at room temperature. The azido-terminated iron magnetic nanoparticles (MP-N_3) were isolated by centrifugation at 12 300 rcf and purified through four consecutive wash/centrifugation cycles at 12 300 rcf with DMF.

MP-N_3 (6 mg in 1 mL of DMF), 4-[(1-oxo-4-pentyn-1-yl)amino]-phenylboronic acid (**1**) (10 mg, 0.0433 mmol), triethylamine (300 μL, 4.3 molar excess), and CuI (1 mg, 0.0052 mmol) were dissolved in 3 mL of DMF and left to stir for 24 h at room temperature. The boronic-acid-terminated iron magnetic nanoparticles (MP-BA) were isolated by centrifugation at 13 500 rcf and purified through consecutive wash/centrifugation cycles at 13 500 rpm with water (twice), 1 mM EDTA (twice), and water (twice).

Nanodiamonds (NDs). 4-Azidobenzoic acid (0.20 mmol), DCC (0.22 mmol), and DMAP (0.066 mmol) were dissolved in 5 mL of anhydrous DMF. A suspension of ND-OH particles in anhydrous DMF (10 mg in 5 mL) was added to the solution and stirred at room temperature for 24 h under nitrogen. The azido-terminated ND particles (ND-N_3) were isolated through consecutive wash/centrifugation at 12 300 rcf with DMF (twice) and ethanol (twice) and finally oven-dried at 50 °C for overnight.

The ND-N_3 (15 mg) were dispersed in 15 mL of anhydrous DMF and sonicated for 40 min. The "click" reaction was carried out by addition of 4-[(1-oxo-4-pentyn-1-yl)amino]phenylboronic acid (**1**) (4 mM) and $CuI(PPh_3)$ (0.4 mM) to the ND-N_3 suspension and stirring the mixture for 48 h at 80 °C. The resulting ND-BAs were separated by centrifugation at 12 300 rcf, purified through consecutive wash/centrifugation cycle at 12 300 rcf with DMF (twice) and 1 mM EDTA water solution (thrice), and finally oven-dried at 50 °C overnight.

Determination of the Amount of Active Boronic Acid on the Nanoparticles. The boronic-acid-modified particles (2 mg) were mixed with 5.5 mM solution of mannose (total volume 1 mL) for 1 h to link the mannose to the boronic acid functions. The amount of linked mannose was determined by treatment with a phenol/H_2SO_4 solution as described previously.[2] First, a calibration curve for mannose in solution was established using a phenolic aqueous solution (5 wt %, 60 μL), concentrated H_2SO_4 (900 μL) which was added to an aqueous mannose solution (60 μL), stirred for 10 min, and then an absorption spectrum was recorded (Perkin-Elmer Lambda 950 dual beam) against a blank sample (without mannose). The absorbance of the solution was measured at two wavelengths: λ_1 = 485 and λ_2 = 570 nm, and the absorbance difference ($A_{485} - A_{570}$) plotted against the concentration of mannose. The quantity of surface-linked mannose was determined with 60 μL of the corresponding particles solution in water (2 mg/mL), treated with phenol/H_2SO_4 following the same protocol as described above.

Instrumentation. *Fourier Transform Infrared Spectroscopy.* Fourier transform infrared (FTIR) spectra were recorded using a ThermoScientific FTIR instrument (Nicolet 8700) with a resolution of 4 cm^{-1}. Dried nanoparticles (1 mg) were mixed with KBr powder (100 mg) in an agate mortar. The mixture was pressed into a pellet under 10 tons load for 2−4 min, and the spectrum was recorded immediately. Sixteen accumulative scans were collected. The signal from a pure KBr pellet was subtracted as a background.

X-ray Photoelectron Spectroscopy. X-ray photoelectron spectroscopy (XPS) measurements were performed in a Specs analysis

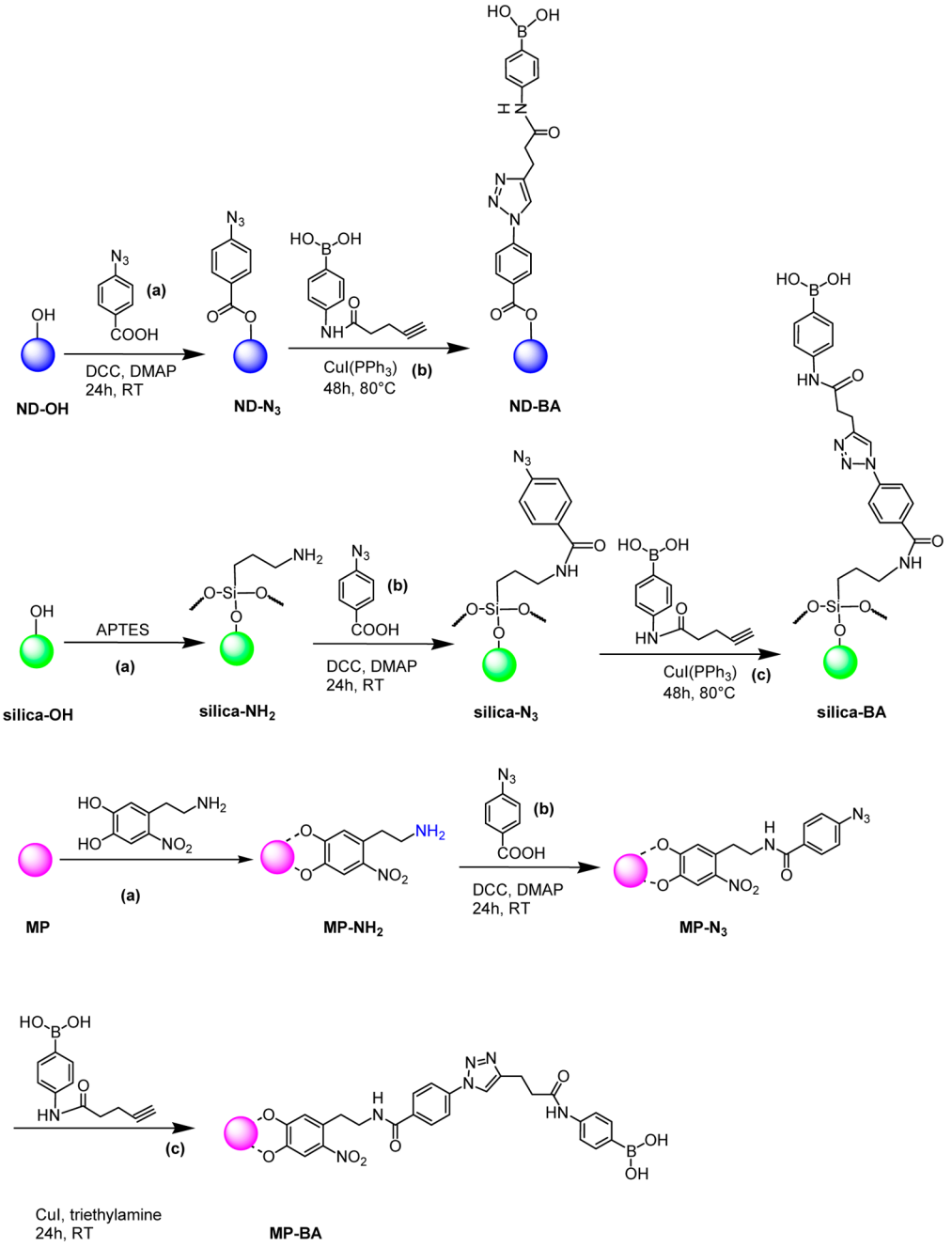

Figure 2. Schematic illustration of the fabrication of boronic-acid-modified nanoparticles.

chamber, equipped with a monochromatized Al Kα X-ray source ($h\nu$ = 1486.74 eV) and a Phoibos 150 mm radius hemispherical electron energy analyzer. The analyzer (constant) pass energy was set to 100 eV for survey spectra and at 20 eV for high resolution scans, with an estimated total (source + analyzer + core hole width) resolution of 0.85 eV for the latter case (for the N 1s spectra). The pressure in the analysis chamber was in 10^{-8} Pa vacuum range, and an electron flood gun operating at 1 eV energy and 100 μA electron current was used to ensure sample neutralization. Electrons are recorded at normal emission in "Large Area Mode" of the Phoibos analyzer. The data presented in Figure 3 are deconvoluted by using mixed Lorentz/Gauss profiles with the CasaXPS software.

Particle Size Measurements. Particle suspensions (40 μg/mL) in water were sonicated. The particle size of the nanoparticles suspensions was measured at 25 °C using a Zetasizer Nano ZS instrument (Malvern Instruments S.A., Worcestershire, U.K.) in 173° scattering geometry, and the zeta potential was measured using the electrophoretic mode.

Biological assays. *Cell Culture.* HuH-7 cells were cultured in Dulbecco's modified Eagle's medium (DMEM, Invitogen) supplemented with 10% heat-inactivated fetal calf serum (FCS, Invitogen), 100 U/mL penicillin, and 100 μg/mL streptomycin (Invitogen).

Cytotoxicity (MTS) Assay. HuH 7 cells were seeded in 96-well plates at a density of 7 × 10^3 cells/well 1 day before assay. The medium was replaced with fresh medium containing the particles of desired concentrations and incubated for 48 h. After that, MTS assay was performed as described by the company (CellTiter 96 AQueous One Solution cell proliferation assay; Promega). First the cells were washed with PBS once, and then cell medium was changed with 20% of MTS solution prepared in fresh medium and incubated for 30−45 min. The optical density of each well was measured using a microplate reader, with absorbance detection at 490 nm. Each condition was

replicated for four times, and wells without particles were taken as negative control.

Virus Entry Inhibition Assay. For experiments with HCV, we used a modified JFH1 virus containing mutations at the C-terminus of the core protein leading to amino acid changes F172C and P173S, which have been shown to increase the viral titers[50] and mutation in E1 glycoprotein to reconstitute the A4 epitope (SSGLYHVTNDC) as described previously.[51] JFH1 virus was preincubated with different concentrations of nanoparticles for 1 h at room temperature. Then the virus/particle complexes were incubated with Huh-7 cells[52] that were seeded at a density of 3×10^4 cells/well 1 day before in 24-well plates containing microscopy coverslip. Two hours later, infected cells were washed two times with PBS to remove complexes completely, and they were further incubated for 48 h with fresh medium. After 48 h, cells were fixed with 100% methanol (−20 °C) and the percentages of infected cells were determined by immunofluorescence using a monoclonal antibody (primary) recognizing HCV glycoprotein E1 (A4 epitope) and likewise secondary antibody carrying fluorophore (CY-3 tagged goat anti-mouse) that recognizes primary antibody .[53] Nuclei were labeled by using 4′-6-diamidino-2-phenylindole (DAPI), a DNA-specific fluorochrome. Infected cells were labeled by CY-3. Five images (for both nucleus and infected cells) were collected from different areas of each coverslip by using a fluorescent microscope (Zeiss Axiophot 2). Further, the total number of cells and infected cells from each image was counted by using Image J. The percentage of infected cells was calculated by using formula below:

$$\%\ \text{infected cells in each condition} = \frac{\text{total no. of infected cells}}{\text{total no. of cells}} \times 100$$

$$\%\ \text{infected cells compared to negative control in each condition} = \frac{\%\ \text{infected cells in each treated condition}}{\%\ \text{infected cells of negative control}} \times 100$$

All the conditions were tested in duplicate. Conditions without particles were taken as negative control.

3. RESULTS AND DISCUSSION

Formation of Boronic-Acid-Modified Nanoparticles. In a previous article relating to boronic-acid-functionalized detonation NDs, the importance of introducing a linker unit between the ND surface and boronic acid functions was demonstrated to have a positive influence on the selectivity of glycoprotein and glycopeptide enrichment.[11,43] The boronolectins described in that study were nevertheless found to be poorly dispersible and prone to interact nonspecifically with nonglycosylated proteins. We have previously reported that mannoside-clicked NDs are very selective for FimH-expressing *E. coli* and observed no unspecific binding of bacteria.[2] In that study, commercially available 4-azidobenzoic acid moieties were attached via their carboxylic acid groups to hydroxyl groups present on the surface of the ND, through an ester linkage. These azide-modified nanostructures were then amenable to a "click" reaction with various propargyl-functionalized ligands. A "click" chemistry approach has also been reported by Zhang et al. for the modification of MPs with boronic acids,[40] and it is thus believed that such a functionalization strategy can be adapted for fabricating boronic-acid-modified silica nanoparticles.[40]

Thus, for detonated hydroxyl-terminated nanodiamonds (ND-OH) (Figure 2), the coupling of 4-azidobenzoic acid units to surface hydroxyl functions proceeded in the presence of *N,N′*-dicyclohexylcarbodiimide (DCC) and a catalytic amount of 4-dimethylaminopyridine to give azide-terminated NDs (ND-N_3), as described before.[2,54] In the case of silica particles (silica-NP-OH) where the surface hydroxyl groups reacted with 4-aminopropyltrimethoxysilane (APTMS) to give the corresponding amine-terminated silica particles (Silica-NP-NH_2), azide-terminated silica particles (silica-NP-N_3) were formed by further reaction with 4-azidobenzoic acid moieties using the DCC protocol. Azide-terminated magnetic particles (MP-N_3) were obtained by first grafting 2-nitrodopamine (**2**) onto the MP surface, followed by conjugation of the thereby introduced amine groups with 4-azidobenzoic acid groups using the DCC protocol. The choice of 2-nitrodopamine for functionalization of MNPs was motivated by the reported irreversible binding of this former ligand compared with that observed for the more commonly used iron oxide ligand, dopamine. This irreversibility is related to the presence of the electronegative nitro group, which leads to enhanced interactions of phenolic functions with the MP surface, leading to its lower rate of oxidation and enhanced stability as compared with dopamine.[55−57] It was also reported that 2-nitrodopamine ligand has pK_a values near pH 6.5, lower when compared to dopamine ligands with pK_a around pH 9.[55−57]

The success of these coupling strategies for establishing a layer of azide groups on the surface of the various nanoparticles was evaluated using both FTIR (Figure 3) and XPS analysis (Figure 4). FTIR transmission spectra of all nanostructures functionalized with 4-azidobenzoic acid are almost identical. These feature a band at 2125 cm^{-1} characteristic of the $\nu_{as(N3)}$ stretching mode, a broad peak at 3447 cm^{-1} assigned to the stretching mode of unreacted surface hydroxyl groups or/and adsorbed water molecules, and a band at 2936 cm^{-1} characteristic of the presence of C−H bonds. In the case of ND-N_3, the band at 1730 cm^{-1} (C═O) confirms the formation of an ester linkage. The band at 1286 cm^{-1} can be attributed to C−O bond stretching on the ND surface, being rather intense when compared to other ND spectra.[58] The FTIR spectrum of MP-N_3 reveals the presence of the 2-nitrodopamine anchor with prominent bands corresponding to C−O and C═C vibrations at 1287 and 1500 cm^{-1} respectively, as well as an intense band at 1548 cm^{-1} ascribable to asymmetric NO_2 group vibrations. In the case of silica-N_3, the bands 1661 and 1643 cm^{-1} characteristic of amides II and I, respectively, are clearly seen in the spectrum of silica-N_3 particles. The absorption corresponding to C−O related bands is not visible, as it is overlapped with the strong stretching vibration of the Si−O−Si groups of silica occurring in the spectral range of 1000−1400 cm^{-1}, with a maximal absorption at ≈1089 cm^{-1}.[59]

The high-resolution N1s XPS spectra of ND-N_3 particles (Figure 4A) reveals unambiguously, the presence of the azido function by the signals at 405.2 (Ar−N═$\underline{N}^+$═N^-) and 401.6 eV (Ar $\underline{N}$═N^+═$\underline{N}^-$) in a ratio of 1:2, as theoretically expected. Additional bands corresponding to azide groups are observed at 399.3 and 402.4 eV with a ratio of 3:1, but these are also characteristic of NH_2 functional groups (399.3 eV) present on the surface of the ND particles and are also found in other nitrogen containing functionalities such as C−N and N−O (402.4 eV), which can be generated from trinitrotoluene during the detonation process. The high-resolution N1s XPS spectra of MPs are somewhat more complex (Figure 4B). The spectrum of nitrodopamine-modified particles (MP-NH_2) shows bands at 404.2 (−$\underline{N}O_2$), 398.2 (−$\underline{N}H_2$), and 400.2 eV (−$\underline{N}H_3^+$). The ratio of NH_2/NO_2 is 2.2 and thus much higher than the theoretically expected one of 1/1. It is however known that NO_2 groups are not stable under XPS conditions (due to

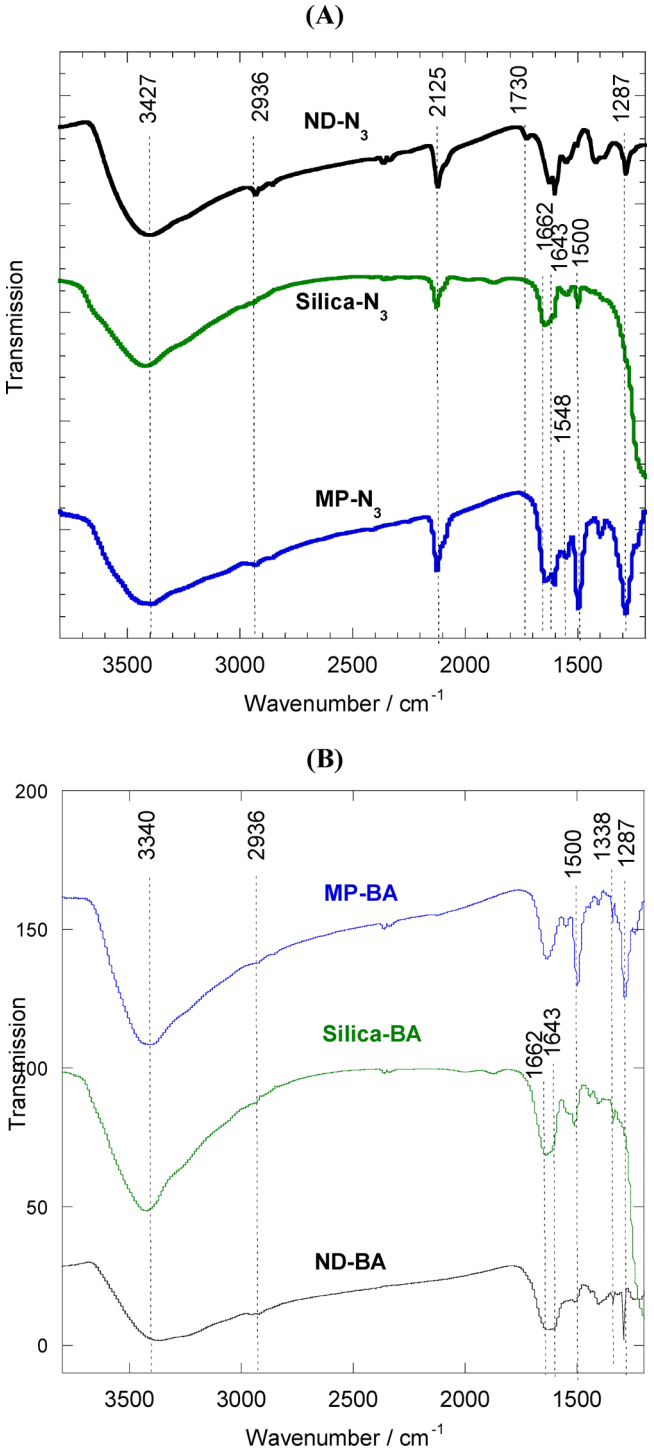

Figure 3. Transmission FTIR spectra of azide-terminated nanoparticles (A) and boronic-acid-modified particles (B).

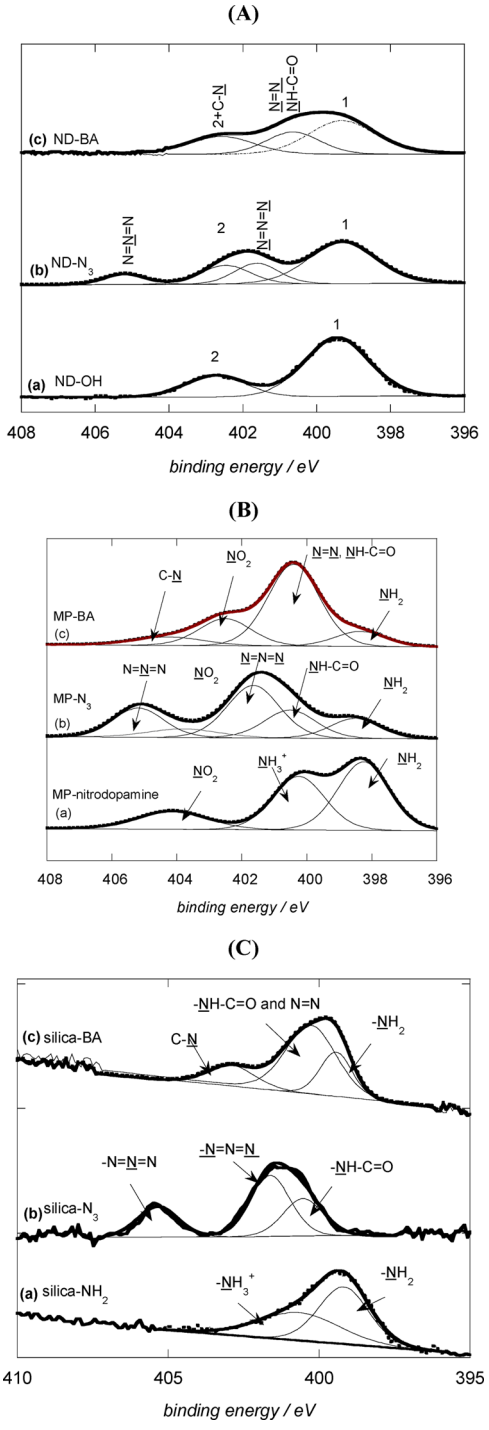

Figure 4. N1s high resolution XPS spectra of the functionalized nanoparticles: (A) (a) ND−OH, (b) ND-N_3, (c) ND-BA. (B) (a) MP-nitrodopamine, (b) MP-N_3, (c) MP-BA. (C) (a) silica-NH_2, (b) silica-N_3, (c) silica-BA.

ultrahigh vacuum conditions, X-ray excitation, and interaction with secondary electrons or with electrons from the flood gun) and can thus be converting into NH_2 groups.[29,60] Upon surface functionalization with 4-azidobenzoic acid moieties, the corresponding XPS spectra of these MP-N_3 shows bands at 405.1 eV (Ar−N═$\underline{N}^+$═N^-) and 401.6 eV (Ar-$\underline{N}$═N^+═$\underline{N}^-$), which are attributable to azido groups. A peak present at 400.5 eV (−NH−C═O linkage) is present in the N1s high-resolution XPS spectra, as are bands at 403.9 and 398.5 eV. The latter are ascribable to $\underline{N}H_2$ groups (formed from $\underline{N}O_2$) as well as residual NH_2 groups whose presence indicates inefficient coupling with 4-azidobenzoic acid. Comparable XPS spectra were generated for silica NPs. The N1s XPS spectrum of silica-NP-NH_2 features bands at 398.2 and 400.2 eV ascribable to $-\underline{N}H_2$ and $-\underline{N}H_3^+$ groups. The N1s high resolution XPS spectrum of the silica-NP-N_3 (Figure 3C) exhibits peaks at 405.3 (Ar−N═$\underline{N}^+$═N^-), 401.5 eV (Ar-$\underline{N}$═N^+═$\underline{N}^-$), and 400.6 eV (−NH−C═O linkage) with a ratio of

dx.doi.org/10.1021/am403770q | ACS Appl. Mater. Interfaces 2013, 5, 12488−12498

Table 1. Physicochemical Characteristics of the Boronic Acid-Modified Nanoparticles

particles	size, nm	ζ-potential, mV (pH 7.4)	BA, μg/mg	BA on 60 μg/mL particles, μg/mL	pK_a
ND-BA	83 ± 2	15.7 ± 0.6	65 ± 2	3.9 ± 0.3	8.0 ± 0.2
MP-BA	93 ± 7	−26.0 ± 0.3	54 ± 2	3.2 ± 0.3	5.0 ± 0.2
silica-BA	100 ± 5	−17.7 ± 0.15	64 ± 5	3.6 ± 0.3	8.0 ± 0.2

1:2:1, in accordance with the chemical composition of the surface.

Having in hand the required NP precursors featuring surface-linked azido groups, we were in a position to fabricate the targeted boronic acid analogues. The propargyl functionalized analogue, 4-[(1-oxo-4-pentyn-1-yl) amino]phenylboronic acid (**1**) was selected as the "click" partner and easily obtained via a modified literature procedure from 4-amino phenylboronic acid chloride and pentynoic acid. When the propargyl analogue (**1**) was subjected to our "standard" click-coupling strategy with each of the NP-N_3 in turn, the expected phenylboronic-acid-clicked NPs (ND-BA, MP-BA, silica-NP-BA) were formed smoothly and efficiently (Figure 2). The successful attachment of boronic acid moieties to NPs is accompanied by simultaneous introduction of surface triazole groups and consequently can be monitored by the disappearance of bands expected for the $\nu_{as(N3)}$ stretching mode at 2123 cm^1 in the FTIR spectra of each of the particles (Figure 3B). The presence of surface boronic acid functions is further evidenced by the stretching mode band of B−O at 1338 cm^{-1} in the FTIR spectra of all successfully clicked particles.[10] Further support for the efficient conversion of surface azide groups into the corresponding triazole functions comes from observation of the absence of the characteristic azide band at 405.2 eV in the N1s XPS spectra of each NP conjugate (Figure 4). The N1s signal of ND-BA and silica-NP-BA can be fitted to bands at 402.6 eV (−C−N−) and 400.4 eV (−N═N−, −NH-C═O), respectively, present in a ratio of 1:3.9 typical of a triazole function. An additional band at 399.2 eV ($-NH_2$) is indicative to the presence of amine groups, perhaps resulting from partial hydrolysis surface azidobenzoic ester functions. In the case of MP-BA, additional bands at 404.19 and 398.5 eV present in its XPS spectra are probably due to the presence of $-\underline{N}O_2$ and $-\underline{N}H_2$ functions at its surface.

It was necessary to quantify the amount of "sugar-accessible" boronic acid functions at the particle surface, as this would be expected to tune the glycan-binding efficiency of a particular NP. The determination of the amount of boronic acid ligands on the surface was performed by an indirect method.[2] Treatment of a given particle with mannose leads to its covalent binding to the NP-BA as a cyclic boronate ester and furnished the corresponding NP saturated with the maximal amount of "bound" sugar. Subsequently, thorough washing of these "sugar-saturated" NPs would remove all unbound mannose. The concentration of particle-attached mannose was then determined using the well-established phenol-sulfuric acid colorimetric assay for the determination of carbohydrate concentration.[61,62] This method of quantifying the surface concentration of boronic acid moieties in effect allows for an estimation of those residues that are actually *available* for binding monosaccharides. Thus, in the assay, the absorption difference between λ = 570 nm (baseline) and λ = 495 nm of an aliquot of a given mannose particle was measured with reference to a calibration curve. This gave sugar loadings of 65 ± 2 μg/mg for ND-BA, 54 ± 2 μg/mg for MP-BA, and 60 ± 5 μg/mg for silica-NP-BA (Table 1). The lower mannose-loading of MP-BA relative to that of other NP conjugates fabricated was somehow surprising. The XPS data for MP-BA (Figure 4B) reveal the presence of residual NH_2 groups, suggesting that the coupling efficiency of surface dopamine groups with 4-azidobenzoic acid was less than optimal and would have resulted in fewer boronic acid groups to be grafted in the subsequent "click" conjugation. While the diameter, and consequently the surface areas, increases in the order ND-BA < MP-BA < silica-BA, it does not to affect the sugar loading as the MP-BA show significantly lower integrated mannose.

The efficiency of the any boronic-acid-modified NPs to "bind" a particular glycan would ultimately be dependent not only on the number of boronic acid residues available for binding sugars but also on their ability to form cyclic diesters with diol functions of sugars at physiological pHs. The majority of boronic acid analogues are weak acids with a pK_a generally in the order of ca. 8−9, when in its anionic form as is the case in alkaline solutions (facilitated by addition of the OH^- ions to the boron atom).[63] Consequently, the surface density of the anionic charges on a particle will be a function of the pH at which it is dispersed and its pK_a value can be determined simply by measuring the variation of its zeta potential as a function of pH. This method has allowed the estimation of pK_a values of 5.0 ± 0.2 for MP-BA and 8.0 ± 0.2 for both ND-BA and silica-BA (summarized in Table 1). The pK_a values observed for the ND-BA and silica-NP-BA are ca. 1 pH unit lower than that expected for a phenylboronic acid without any substitution on the aromatic ring. The latter compounds usually show values for pK_a's of ca. 8.8 and therefore bind strongly to diols only at alkaline pHs.[17] Multivalent presentation of boronic acid units[64] as well as dative bond formation with boron[18,24,25] and the addition of electron-withdrawing groups on the phenyl ring of the phenylboronic acid[17,64] have all been found to decrease the pK_a and thus improve binding of diols at physiological pHs compared to that seen for unsubstituted phenylboronic acid. In the case of the ND-BA and silica-BA, the presence of multiple triazole functions and of residual surface OH groups is expected to favor intermolecular interaction of accessible nitrogen and oxygen functions with adjacent boronic acid groups and facilitate a decrease in the effective macroscopic pK_a's. However, the presence of multiple boronic acids would not be expected to wholly account for the unexpectedly low pK_a value observed for the MP-BA. It might be conjectured that this observation might be related to the presence in MP-BA particles of the electron-withdrawing nitro group in 2-nitrodopamine (incorporation of electron withdrawing groups onto phenylboronic acid derivatives is known to lower their pK_a[65]) as well as the observation that residual unreacted amine groups are present on its surface (boronic acids are known to be prone to dative bond formation with adjacent nitrogen or oxygen ligands resulting in lowering of their effective pK_a).[66,67]

Effect of Nanoparticles on Huh-7 Cell Viability. Trace copper is known to be toxic for various human cell lines,[68] and we thought to ensure complete removal of contaminant copper residues remaining after the azide−alkyne Huisgen cyclo-addition reaction. This was conveniently achieved through

introducing three aqueous EDTA washing/centrifugation cycles into the post-"click" treatment of all conjugated particles prior to their being used in cell-based assays. XPS analysis of these NPs confirmed the absence of any copper traces and confirmed to some extent the purity of the NPs before being subjected for biological evaluation. That such a washing protocol is efficient to perform biological tests was recently demonstrated by the study of biofilm inhibition assays in the presence of ND modified by "click" chemistry with mannose units.[2] The cell viability of each of the boronic-acid-modified NPs was established on the Huh-7 cell line after 48 h incubation, to be used in the subsequent HCV-entry inhibition experiments. At the highest concentration of ND-BA and MP-BA particles (80 μg/mL), no substantial reduction in the viability of Huh-7 cells was observed (Figure 5). The observed lack of cytotoxicity

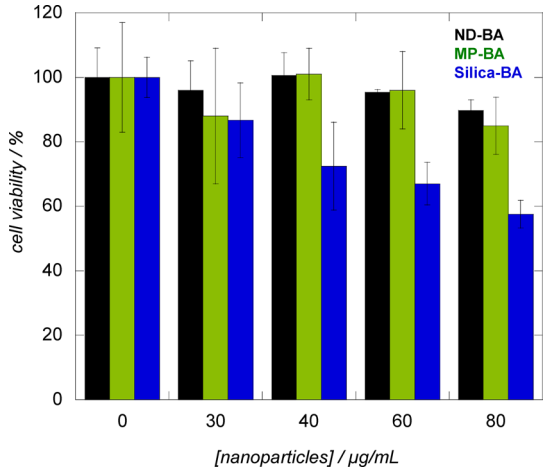

Figure 5. HuH-7 cell viability results after 48 h incubation using nanoparticles of different concentration: ND-BA (black), MP-BA (green), silica-BA (blue).

is in accordance with previous studies demonstrating the excellent biocompatibility of these NDs.[69,70] That iron-containing nanoparticles are biocompatible would be expected in that iron is present in the human body (ferritin) as our routes for its eventual elimination.[71] In addition, coating MPs with nitrodopamine would be expected to increase their stability and thus their cell viability. The silica-NP-BA particles show, on the other hand, a higher reduction in the viability of Huh-7 cells than the other NP-BAs. The toxicity of silica-NPs is highly dependent on the physical, chemical and structural properties of a particular particle formulation.[72−74] However, in the HCV inhibition experiments (see below, Figure 6A), NP-BA particles are only exposed to Huh-7 target cells for a period of 2 h and, on this time scale, silica-NP-BAs do not show any cytotoxicity effects (data not shown).

Inhibition of HCV Infection by Boronic-Acid-Modified NPs. An assay that measures the ability of this cell-culture-derived JFH1 virus to infect hepatocytes was applied to evaluate the potential of each boronic-acid-modified NP as an inhibitor of viral entry. The modified JFH1 virus featuring mutations shown to increase the viral titers was used in experiments with HCV.[50] The various steps of the assay are shown schematically in Figure 6A. Thus, serially increasing concentrations of a given particle were mixed with a fixed quantity of modified JFH1 virus and incubated for 1 h before the mixture was brought into contact with a fixed number of Huh-7 target cells. Upon incubation for 48 h, the number of infected cells at each dilution was quantified by immunofluorescence. Figure 6B shows typical fluorescence images of the Huh-7 target cells after being incubated with modified JFH1 virus for 48 h, in the presence of various nanostructures including those modified with boronic acid moieties. The red colored cells are those that have been infected. In this assay, the ND-BA particles showed viral inhibition of up to 58 ± 10% (Figure 6C) for particle concentrations of 60 μg/mL, corresponding to 3.9 μg/mL of available boronic acid units (Table 1). Unmodified particles, when subjected to the same assay conditions, did not inhibit HCV infection even at high concentrations. A somewhat lower viral inhibition efficiency (≈47 ± 8%) than seen with other NP-conjugates was seen for MP-BAs, an observation related possibly to their lower available boronic acid content. The best results were obtained for silica-NP-BA particles. At a concentration of 60 μg/mL, NPs, the viral inhibition was 60 ± 8%. The use of higher concentrations of any of the NP-BAs did not lead to any enhancement of their antiviral effects (data not shown). We consider this to be linked to formation of NP-derived precipitates at these elevated concentrations during the assay.

An additional control experiment was performed to establish that only NPs featuring multiply presented boronic acid moieties have an effect on HCV, the effect of free boronic acid derivative (**1**) at concentrations of between 0 and 25 μg/mL was examined under identical assay conditions to those used for the NPs (Figure 7A). No antiviral effect was observed with the monovalent analogue. Furthermore, when ND-BA particles were saturated with mannose prior to their incubation with the viral particles, they showed no antiviral activity (Figure 7B). This experiment confirmed that masking of the mannose-binding function of ND-BAs (and other particles studied) resulted in the loss of antiviral activity and further that the antiviral activity was dependent on boronic cyclic diester formation between the particle-appended boronic acid moieties and glycoproteins present on HCV envelope.

4. CONCLUSIONS

A comparative study of the utility of three different nanoparticles featuring surface-attached boronic acid moieties as synthetic viral entry inhibitors was undertaken. We demonstrate that iron-, silica-, and diamond-derived NPs manifest viral entry inhibitory activity against HCV in vitro. While silica NPs were the least biocompatible, they showed the best inhibition of HCV entry. These synthetic NP-conjugates may be considered as functional analogues of the natural lectins cyanovirin-N and griffithsin, both of which have been shown in vitro as well as in vivo to elicit viral entry inhibition through their ability to interact with high-mannose glycans present on HCV envelope glycoproteins. The advantage over other HCV inhibition agents is the facility with which the described nanostructures have been fabricated, their low cost (compared with lectins for example), and high quantity using the Cu(I) click conjugation strategy described here. Moreover, it is shown that the activity of the newly fabricated borono-lectins is due to the presence on their surfaces of multiple boronic acid residues rather than nonselective effects of unmodified NPs using an assay which measures the potential of cell culture-derived JFH1 virus to infect hepatocytes. While the reduction of HCV infection of these first generation boronic-acid-derived NPs is still modest (around 40%), the results nevertheless provide strong evidence that such entities might be further improved and developed as a

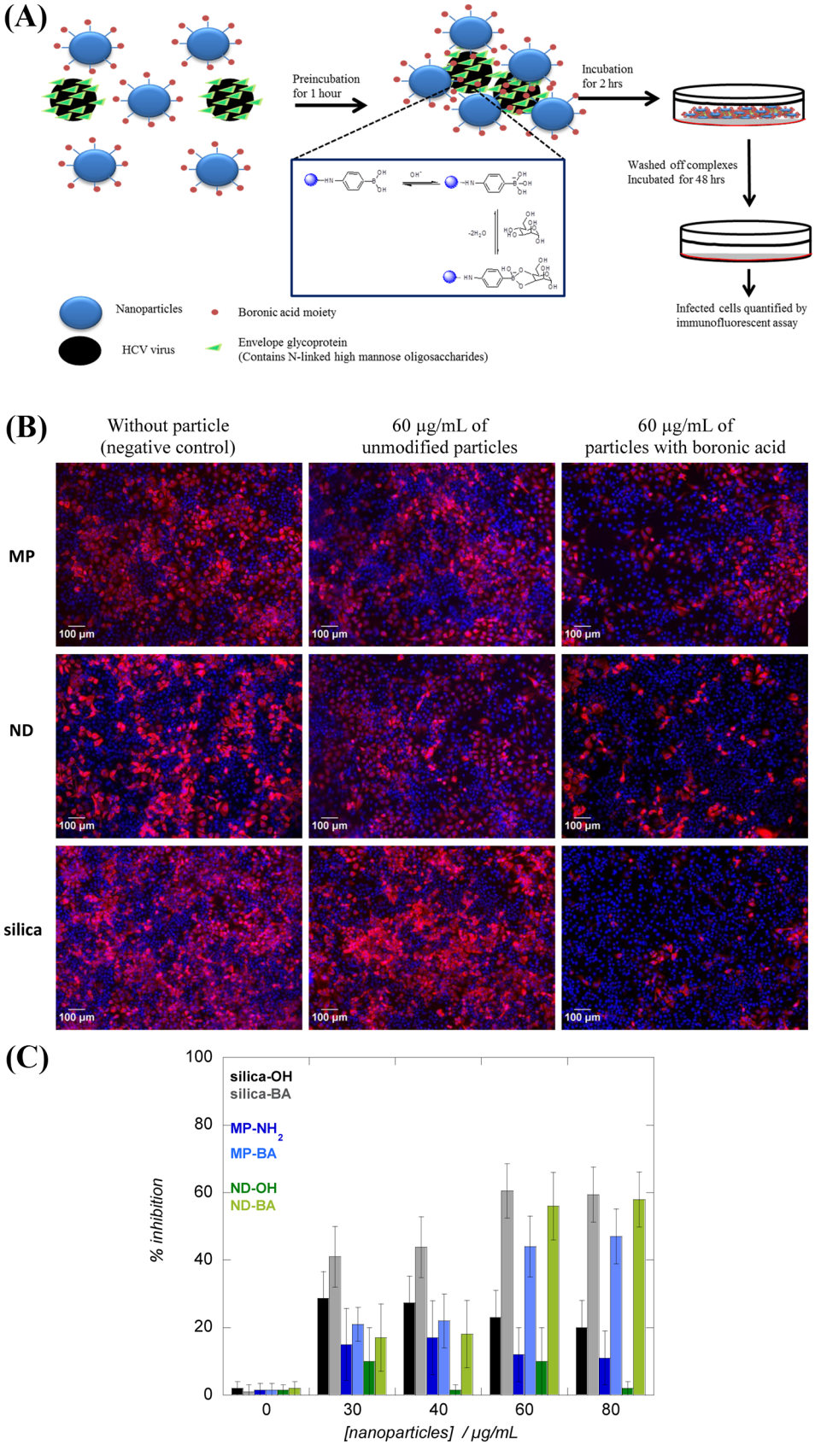

Figure 6. (A) Graphical depiction of performed antiviral assay. (B) Fluorescent image (10×) of the Huh-7 target cells after incubation with modified JFH1 virus for 48h, incubation in the presence of the nanostructures and boronic-acid-modified nanostructures, along with absence of any nanostructures (red color and blue color correspond to infected cells and nucleus, respectively). (C) Effect of particle concentration in the entry inhibition activity: silica-OH (black), silica-BA (gray), MP-NH_2 (dark blue), MP-BA (light blue), ND-OH (green), ND-BA (light green).

dx.doi.org/10.1021/am403770q | *ACS Appl. Mater. Interfaces* 2013, 5, 12488−12498

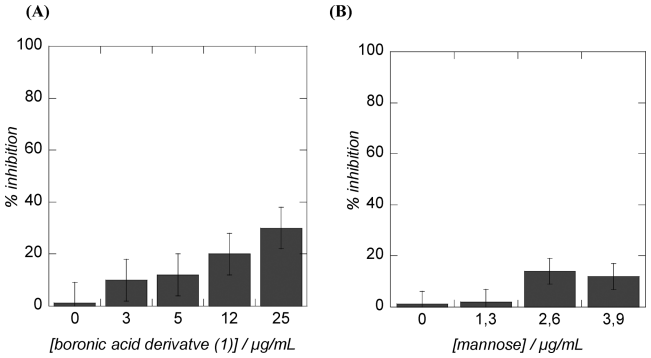

Figure 7. (A) Effect of concentration of boronic acid derivative (**1**) on the entry inhibition activity. (B) Effect of mannose blocking of BA functions on ND-BA on the viral entry inhibition activity.

viral entry inhibition strategy of HCV. Furthermore, in principle, the infectivity of any other pathogens that feature cell wall glycoproteins that are essential for their life cycle might also be reduced using similar NP-based boronolectins. That the newly developed borono-lectins described here manifest a lower cellular toxicity than alternative nanomaterials, sets the stage for the further exploration of NP-based pseudolectins as alternatives to their natural lectin counterparts. The study also supports that NP-derived borono-lectins should be further developed and pursued as a potential therapeutic strategy for blocking viral entry of HCV.

AUTHOR INFORMATION

Corresponding Authors

*E-mail: aloysius.siriwardena@u-picardie.fr.
*E-mail: jean.dubuisson@ibl.fr.
*E-mail: Sabine.Szunerits@iri.univ-lille1.fr.

Notes

The authors declare no competing financial interest.

ACKNOWLEDGMENTS

M.K., A.B., R.B., and S.S. gratefully acknowledge financial support from the Centre National de Recherche Scientifique (CNRS), the Université Lille 1, and the Nord Pas de Calais region. T.V. and J.D. were supported by a grant from the French National Agency for Research on AIDS and Viral Hepatitis (ANRS). Support from the European Union through a FP7-PEOPLE-IRSES (PHOTORELEASE) is acknowledged. M.K. gratefully acknowledges financial support from the Nord Pas de Calais region for a Ph.D. fellowship. Support from the CEIFPRA-ICPAR is acknowledged by O.B. and A.S. We thank T. Wakita for providing us with JFH1 infectious clone. The fluorescence microscopy data were generated with the help of the Bioimaging Center Lille Nord-de-France (BICeL). N.G.A. and C.M.T. acknowledge the PCA 128/2012 Project, granted by the Romanian UEFISCDI Agency.

REFERENCES

(1) Sapsford, K. E.; Algar, W. R.; Berti, L.; Boeneman Gemmill, K.; Casey, B. J.; Oh, E.; Stewaft, M. H.; Medintz, I. L. *Chem. Rev.* **2013**, *113*, 1904−2074.
(2) Barras, A.; Martin, F. A.; Bande, O.; Baumann, J. S.; Ghigo, J.-M.; Boukherroub, R.; Beloin, C.; Siriwardena, A.; Szunerits, S. *Nanoscale* **2013**, *5*, 2307−2316.
(3) Krüger, A.; Lang, D. *Angew. Chem., Int. Ed.* **2010**, *22*, 890−906.
(4) Turcheniuk, K.; Boukherroub, R.; Szunerits, S. *Nanoscale* **2013**, *5*, 10729−10752.
(5) Compain, P.; Decroocq, C.; Iehl, J.; Holler, M.; Hazelard, D.; Barragan, T. M.; Mellet, C. O.; Nierengarten, J.-F. *Angew. Chem., Int. Ed.* **2010**, *122*, 5889−5892.
(6) Trippier, P. C.; McGuigan, C. *Med. Chem. Commun.* **2010**, *1*, 183−198.
(7) Hosmane, N. S. *Boron Sciencec: New Technologies and Applications*; CRC Press: Boca Raton, FL, 2012.
(8) Yan, J.; Fang, H.; Wang, B. *Med. Res. Rev.* **2005**, *25*, 490−520.
(9) Yeap, W. S.; Tan, Y. Y.; Loh, K. P. *Anal. Chem.* **2008**, *80*, 4659−4665.
(10) Lin, Z.-A.; Zhend, J.-N.; Lin, F.; Zhang, L.; Cai, Z.; Chen, G.-N. *J. Mater. Chem.* **2011**, *21*, 518−524.
(11) Xu, Y.; Wu, Z.; Zhang, L.; Lu, H.; Yang, P.; Webley, P. A.; Zhao, D. *Anal. Chem.* **2009**, *81*, 503−508.
(12) Tang, J.; Liu, Y.; Qi, D.; Yao, G.; Deng, C.; Zhang, X. *Proteomics* **2009**, *9*, 5046−5055.
(13) Takahashi, D.; Hirono, S.; Toshima, K. *Chem. Commun.* **2011**, *47*, 11712−11714.
(14) Zhao, Y.; Trewyn, B. G.; Slowing, I. I.; Lin, V. S.-Y. *J. Am. Chem. Soc.* **2009**, *131*, 8398−8400.
(15) Wiskur, S. L.; Lavigne, J. L.; Metzger, A.; Tobey, S. L.; Lynch, V.; Anslyn, E. V. *Chem.—Eur. J.* **2004**, *10*, 3792−3804.
(16) Springsteen, G.; Wang, B. H. *Tetrahedron* **2002**, *58*, 5291−5300.
(17) Yan, J.; Springsteen, G.; Deeter, S.; Wang, B. *Tetrahedron* **2004**, *60*, 11205−11209.
(18) Cai, S. X.; Keana, J. F. W. *Bioconjugate Chem.* **1991**, *2*, 317−322.
(19) Dawlut, M.; Hall, D. G. *J. Am. Chem. Soc.* **2006**, *128*, 4226−4227.
(20) Balzarini, J. *Nat. Rev. Microbiol.* **2007**, *5*, 583−597.
(21) Balzarini, J. *Lancet Infect. Dis.* **2005**, *5*, 726−731.
(22) Trippier, P. C.; Balzarini, J.; McGuigan, C. *Antiviral Chem. Chemother.* **2011**, *21*, 129−142.
(23) Trippier, P. C.; McGuigan, C.; Balzarini, J. *Antiviral Chem. Chemother.* **2010**, *20*, 249−257.
(24) Jay, J. I.; Lai, B. E.; Myszka, D. G.; Mahalingam, A.; Langheinrich, K.; Katz, D. F.; Kiser, P. F. *Mol. Pharmaceutics* **2009**, *7*, 116−129.
(25) Mahalingam, A.; R., G. A.; Balzarini, J.; Kiser, P. F. *Mol. Pharmaceutics* **2011**, *8*, 2465−2475.
(26) Helle, F.; Vieyres, G.; Elkrief, L.; Popescu, C.-L.; Wychowski, C.; Descamps, V.; Castelain, S.; Roingeard, P.; Duverlie, G.; Dubuisson, J. *J. Virol.* **2010**, *84*, 11905−11915.
(27) Anjum, S.; Wahid, A.; Afzal, M. S.; Albecka, A.; Alsaleh, K.; Tahir, A.; Baumert, T.; Wychowski, C.; Qadri, I.; Penin, F.; Dubuisson, J. *J. Infect. Dis.* **2013**, in press.
(28) Grundner, C.; Pancera, M.; Kang, J. M.; Koch, M.; Sodroski, J.; Wyatt, R. *Virology* **2004**, *330*, 233−248.
(29) Lavanchy, D. *Clin. Microbiol. Infect.* **2011**, *17*, 107−115.
(30) Ploss, A.; Dubuisson, J. *Gut* **2012**, *61*, i25−35.
(31) Meuleman, P.; Albecka, A.; Belouzard, S.; Vercauteren, K.; Verhoye, L.; Wychowski, C.; Leroux-Roels, G.; Palmer, K. E.; Dubuisson, J. *Antimicrob. Agents Chemother.* **2011**, *55*, 5159−5167.
(32) Takebe, Y.; Saucedo, C. J.; Lund, G.; Uenishi, R.; Hase, S.; Tsuchiura, T.; Kneteman, N.; Ramessar, K.; Tyrrell, D. L.; Shirakura, M.; Wakita, T.; McMahon, J. B.; O'Keefe, B. R. *PLoS One* **2013**, *8*, e64449.
(33) Helle, F.; Wychowski, C.; Vu-Dac, N.; Gustafson, K. R.; Voiseet, C.; Dubuisson, J. *J. Biol. Chem.* **2006**, *281*, 25177−25183.
(34) Kubik, S. *Angew. Chem., Int. Ed.* **2009**, *48*, 1722−1725.
(35) Davis, A. P. *Biomol. Chem.* **2009**, *7*, 3629−3638.
(36) Alhaddad, A.; Adam, M. P.; Botsoa, J.; Dantelle, G.; Perruchas, S.; Gacoin, T.; Mansuy, C.; Lavielle, S.; Malv, y. C.; Treussart, F.; Bertrand, J. R. *Small* **2011**, *4*, 3087−3095.
(37) Moore, L.; Chow, E. K.; Osawa, E.; Bishop, J. M.; Ho, D. *Adv. Mater.* **2013**, *12*, 3532−3541.
(38) Mohan, N.; Che, C.-S.; Hsieh, H.-H.; Wu, Y.-C.; Chang, H.-C. *Nano Lett.* **2010**, *10*, 3692−3699.

(39) Chow, E. K.; Zhang, X.-Q.; Chen, M.; Lam, R.; Robinson, E.; Huang, H.; Schaffer, D.; Osawa, E.; Goga, A.; Ho, D. *Sci. Transl. Med.* **2011**, *3*, 73ra21.
(40) Zhang, X.; He, X.; Chen, L.; Zhang, Y. *J. Mater. Chem.* **2012**, *22*, 16520−16526.
(41) Lin, Z.; Zheng, J.; Xia, Z.; Yang, H.; Zhang, L.; Chen, G. *RSC Adv.* **2012**, *2*, 5062−5065.
(42) Berube, M.; Dowlut, M.; Hall, D. G. *J. Org. Chem.* **2008**, *73*, 6471−6479.
(43) Xu, Y.; Zhang, W.; Wei, L.; Lu, H.; Yang, P. *Analyst* **2013**, *138*, 1876−1885.
(44) Kolb, H. C.; Finn, M. G.; Sharpless, K. B. *Angew. Chem., Int. Ed.* **2001**, *40*, 2004−2021.
(45) Sapsford, K. E.; Algar, W. R.; Berti, L.; Boeneman Gemmill, K.; Casey, B. J.; Oh, E.; Stewart, M. H.; Medintz, I. L. *Chem. Rev.* **2013**, *113*, 1904−2074.
(46) Wang, Y.; Xiao, Y.; Tan, T. T. Y.; Ng, S.-C. *Tetrahedron Lett.* **2008**, *49*, 5190.
(47) Kanayama, N.; Kitano, H. *Langmuir* **2000**, *16*, 577−583.
(48) Rodenstein, M.; Zürcher, S.; Tosatti, S. G.; Spencer, N. D. *Langmuir* **2010**, *26*, 16211−16220.
(49) Mazur, M.; Barras, A.; Kuncser, V.; Galantanu, A.; Zaitzev, V.; Turcheniuk, K.; Woisel, P.; Lyskawa, J.; Laure, W.; Siriwardena, A.; Boukherroub, R.; Szunerits, S. *Nanoscale* **2013**, *5*, 2692−2702.
(50) Delgrange, D.; Pillez, A.; Castelain, S.; Cocquerel, L.; Rouillé, Y.; Dubuisson, J.; Wakita, T.; Duverlie, G.; Wychowski, C. *J. Gen. Virol.* **2007**, *88*, 2495−2503.
(51) Goueslain, L.; Alsaleh, K.; Horellou, P.; Roingeard, P.; Descamps, V.; Duverlie, G.; Ciczora, Y.; Wychowski, C.; Dubuisson, J.; Rouillé, Y. *J. Virol.* **2010**, *84*, 773−787.
(52) Nakabayashi, H.; Taketa, K.; Miyano, K.; Yamane, T.; Sato, J. *Cancer Res.* **1982**, *42*, 3858−3863.
(53) Dubuisson, J.; Hsu, H. H.; Cheung, R. C.; Greenberg, H. B.; Russell, D. G.; Rice, C. M. *J. Virol.* **1994**, *68*, 6147−6160.
(54) Barras, A.; Szunerits, S.; Marcon, L.; Monfilliette-Dupont, N.; Boukherroub, R. *Langmuir* **2010**, *26*, 13168−13172.
(55) Amstad, E.; Gehring, A. U.; Fisher, H.; Nagaiyanallur, V. V.; Hähner, G.; Textor, M.; Reimhult, E. *J. Phys. Chem. C* **2011**, *115*, 683−691.
(56) Amstad, E.; Gillich, T.; Bilecka, I.; Textor, M.; Reimhult, E. *Nano Lett.* **2009**, *9*, 4042−4048.
(57) Amstad, E.; M., T.; Reimhult, E. *Nanoscale* **2011**, *3*, 2819−2843.
(58) Yeap, W. S.; Chen, S.; Loh, K. P. *Langmuir* **2009**, *25*, 185−191.
(59) Zhang, L.; Xu, Y.; Yao, H.; Xie, L.; Yao, J.; Lu, H.; Yang, P. *Chem.—Eur. J.* **2009**, *15*, 10158−10166.
(60) Iqbal, P.; Critchley, K.; Attwood, D.; Tunnicliffe, D.; Evans, S. D.; Preece, J. A. *Langmuir* **2008**, *16*, 13969−13976.
(61) Wang, X.; Ramstrom, O.; Yan, M. *J. Mater. Chem.* **2009**, *19*, 8944−8949.
(62) Durka, M.; Buffet, K.; Iehl, J.; Holler, M.; Nierengarten, J. F.; Taganna, J.; Bouckaert, J.; Vincent, S. P. *Chem. Commun.* **2011**, *47*, 1321−1323.
(63) Takahshi, S.; Anzai, J.-I. *Langmuir* **2005**, *21*, 5102−5107.
(64) Kaur, G.; Fang, H.; Gao, X.; Li, H.; Wang, B. *Tetrahedron* **2006**, *62*, 2583−2589.
(65) Matsumoto, A.; Yamamato, K.; Yoshida, R.; Kataoka, K.; Aoyagi, T.; Miyahara, Y. *Chem. Commun.* **2010**, *46*, 2203−2205.
(66) Wulff, G. *Pure Appl. Chem.* **1982**, *54*, 2093−2102.
(67) Wulff, G.; Lauer, M.; Bohnke, H. *Angew. Chem., Int. Ed.* **1984**, *23*, 741−742.
(68) Tardito, S.; Bassanetti, I.; Bignardi, C.; Elviri, L.; Tegoni, M.; Mucchino, C.; Bussolati, O.; Franchi-Gazzola, R.; Marchio, L. *J. Am. Chem. Soc.* **2011**, *133*, 6235−6242.
(69) Schrand, A. M.; Huang, H.; Carlson, C.; Schlager, J. J.; Osawa, E.; Hussain, S. M.; Dai, L. *J. Phys. Chem. B* **2007**, *111*, 2−7.
(70) Marcon, L.; Riquet, F.; Vicogne, D.; Szunerits, S.; Bodart, J.-F.; Boukherroub, R. *J. Mater. Chem.* **2010**, *20*, 8064−8069.
(71) Markides, H.; Rotherham, M.; Haj, A. J. E. *J. Nanomater.* **2012**, *2012*, 614094.
(72) Bauer, A. T.; Strozyk, E. A.; Gorzelanny, C.; Westerhausen, C.; Desch, A.; Schneider, M. F.; Schneider, S. W. *Biomaterials* **2011**, *32*, 8385−8593.
(73) McCarthy, J.; Stepniak, I. I.; Corbalan, J. J.; Radomski, M. W. *Chem. Res. Toxicol.* **2012**, *25*, 2227−2237.
(74) Yu, T.; Malugin, A.; Chandehari, H. *ACS Nano* **2011**, *5*, 5717−5728.

NOTE ADDED AFTER ASAP PUBLICATION

This paper was published on the Web on November 19, 2013, with a spelling error in an author name. The corrected version was reposted on November 27, 2013.